LA-3478 Part II

c. 1

LOS ALAMOS SCIENTIFIC LABORATORY
of the
University of California

LOS ALAMOS • NEW MEXICO

Time-of-Flight Neutron Cross Section Measurements Using Nuclear Explosions (Part II)

UNITED STATES
ATOMIC ENERGY COMMISSION
CONTRACT W-7405-ENG. 36

This report expresses the opinions of the author or authors and does not necessarily reflect the opinions or views of the Los Alamos Scientific Laboratory.

Printed in the United States of America. Available from
Clearinghouse for Federal Scientific and Technical Information
National Bureau of Standards, U. S. Department of Commerce
Springfield, Virginia 22151
Price: Printed Copy $3.00; Microfiche $0.65

LA-3478 Part II
UC-34, PHYSICS
TID-4500

LOS ALAMOS SCIENTIFIC LABORATORY
of the
University of California
LOS ALAMOS • NEW MEXICO

Report written: December 20, 1966
Report distributed: March 20, 1967

Time-of-Flight Neutron Cross Section Measurements Using Nuclear Explosions (Part II)

by

P. A. Seeger
D. W. Bergen

Abstract

The procedures used for converting analog (film) records of data obtained from the interaction of nuclear-device-produced neutrons with target nuclei to cross section as a function of neutron energy are described. A discussion of the errors is also presented.

The conversion procedures include digitizing the records; converting all data to signal, S(t), vs time; deriving a background to be subtracted from all signals; deriving a flux based on the known cross section of a foil isotope; and obtaining the cross section by converting signal to reaction rate and dividing by the flux and foil density.

Table of Contents

I. Introduction

Part I of this report[1] deals with the experimental considerations and procedures involved in recording cross-section data obtained from a very high-intensity single-pulsed neutron source. This part describes in detail the reduction of these photographic film records to neutron cross sections as a function of energy.

The data reduction takes place in three steps. First, the analog information recorded on film is digitized and rendered suitable for computer usage. This step includes reading of both signal and calibration information and editing onto magnetic tape. Such a tape contains X-Y coordinates (in arbitrary units) of points on the signal and on the calibration of a given trace. Second, the calibrations are used to reduce the data to the form signal (millivolts) vs time (microseconds). This is accomplished by locating the position of each point of the signal trace with respect to the stair-step calibration signal and with respect to the uniform time marks, all of which are recorded on the same film. Third and finally, each signal must be compared to the signal from a target with known cross section (^{6}Li or ^{235}U in appropriate energy ranges), taking into account geometrical differences and target compositions, to obtain cross section vs energy. In this process a time varying background recorded from a detector viewing a blank foil backing is subtracted from each signal, and the neutron flux is derived from the reference signal.

II. Digitization

A. Description of Film Records

Three types of film records have been used for recording data. For simplicity these are classed as streak, raster, and plate.

Figure 1 displays typical signals for the streak mode of recording, in which the oscilloscope dot is displaced by the signal in only one dimension, transverse to the direction of film travel, and the time base is provided by the film motion itself. Six data signals were recorded on this film, from three dual-beam oscilloscopes. An additional small cathode-ray tube was used to give a baseline reference line (fifth trace from the bottom). Time marks from a crystal-controlled 20-μsec raster generator are imposed upon the reference trace. The total length of film shown in Fig. 1 is 10 cm; in order to realize the time resolution of 1 μsec inherent in this recording mode, readings of time coordinates must be spaced finer than 30 μm on the film. The vertical gain of the system, including logarithmic amplifiers, oscilloscopes, and cameras, is approximately 600 μm/decade; in order to obtain a signal resolution of 1% or ± 0.0044 in the $\log_{10}$, the resolution of the film digitization must be 2.6 μm. Figure 2 shows the 8-step staircase calibrations for some of the signals on this film, recorded beginning 15 msec after the signal. A commutator was used to calibrate one amplifier every millisecond to the end of the film, providing about five calibrations for each amplifier.

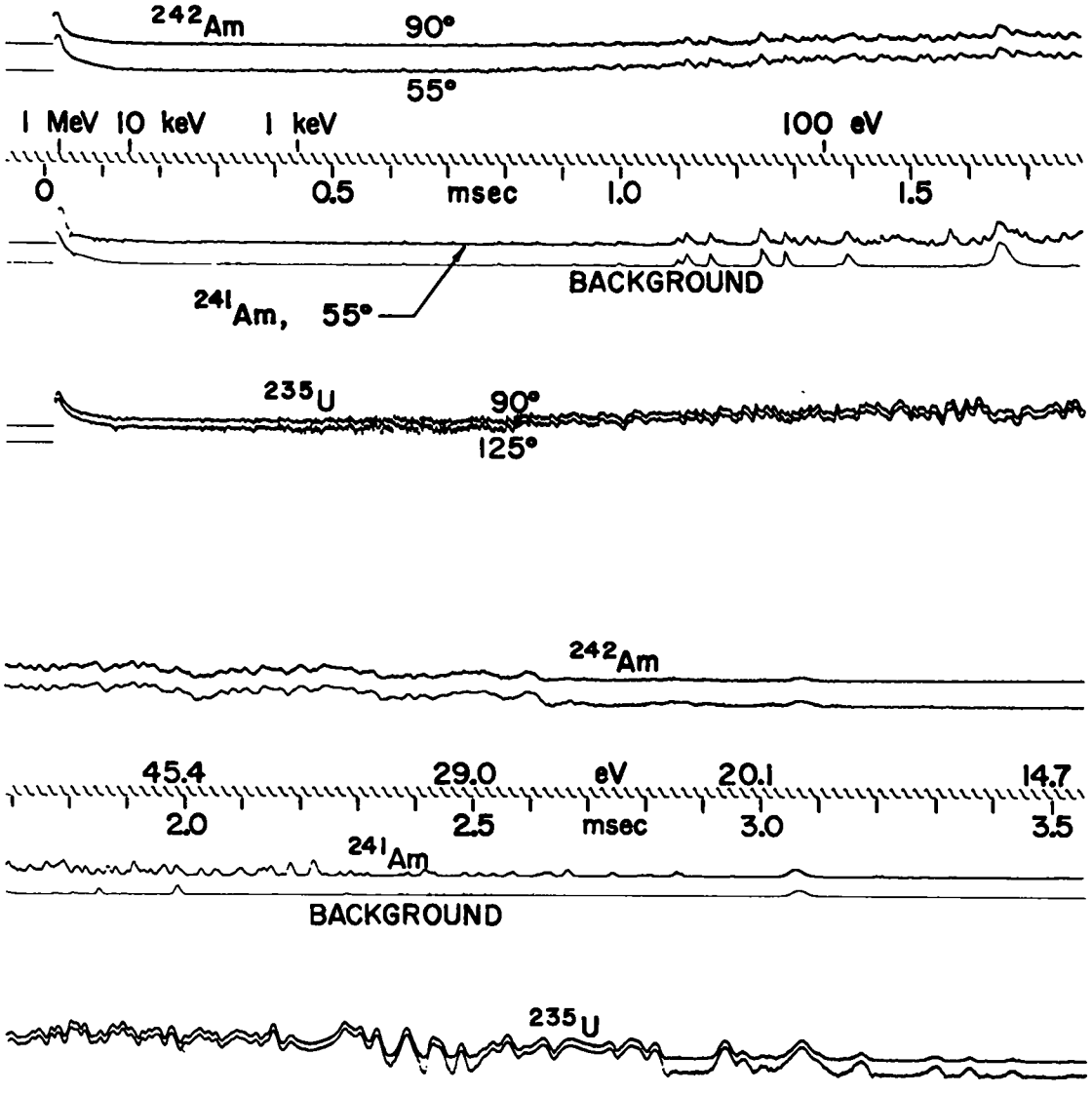

Fig. 1. Streak mode signals.

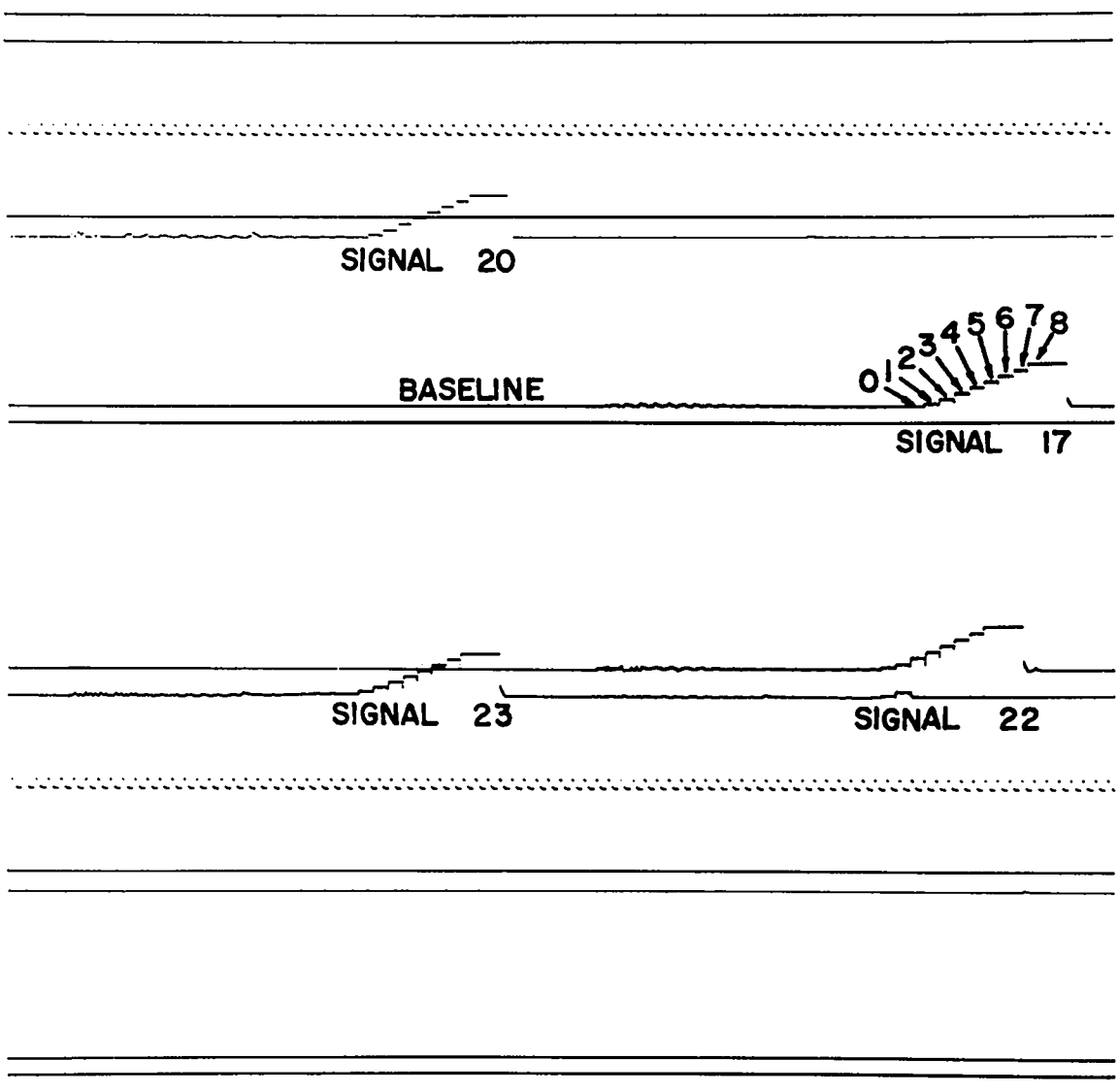

Fig. 2. Calibrations for streak mode signals.

Figure 3 displays a small portion (2.5 cm) of a typical film recorded in the raster mode, in which the time-base is provided by a free-running crystal-controlled 20-μsec saw-tooth generator, and the repetitive sweeps are separated on the film by the continuous motion of the film, which also slants the sweeps. The data signal deflects the beam in opposition to film motion. Four signals (two dual-beam oscilloscopes) are shown, along with the baseline reference signal which is derived from the sweep generator and which, therefore, reveals the position of the baseline for each sweep by comparison to the baseline recorded before the data signal begins. To obtain resolutions of 0.1 μsec and 1% signal, film reading resolutions of 20 μm in the time direction and 2 μm in the signal direction are required. The upper half of Fig. 4 shows an example of the 8-step calibration signal superimposed on square-wave time marks; a single-beam oscilloscope is shown for simplicity. The lower part of Fig. 4 illustrates how readings of the corners (circled points on "baseline" sweep) provide a two-dimensional map of the oscilloscope face.

Some duplicate records were also made on plate film from triggered single-sweep oscilloscopes with various delays and sweep lengths. Because timing and calibration information was not included on the shot film, these records were used only where they could be normalized to other data. Analysis is the same as for streak records.

B. Semi-Automatic Film Reading

Semi-automatic readers are defined here as that class of equipment upon which an operator visually aligns a cursor with the point to be digitized and then causes a digitized

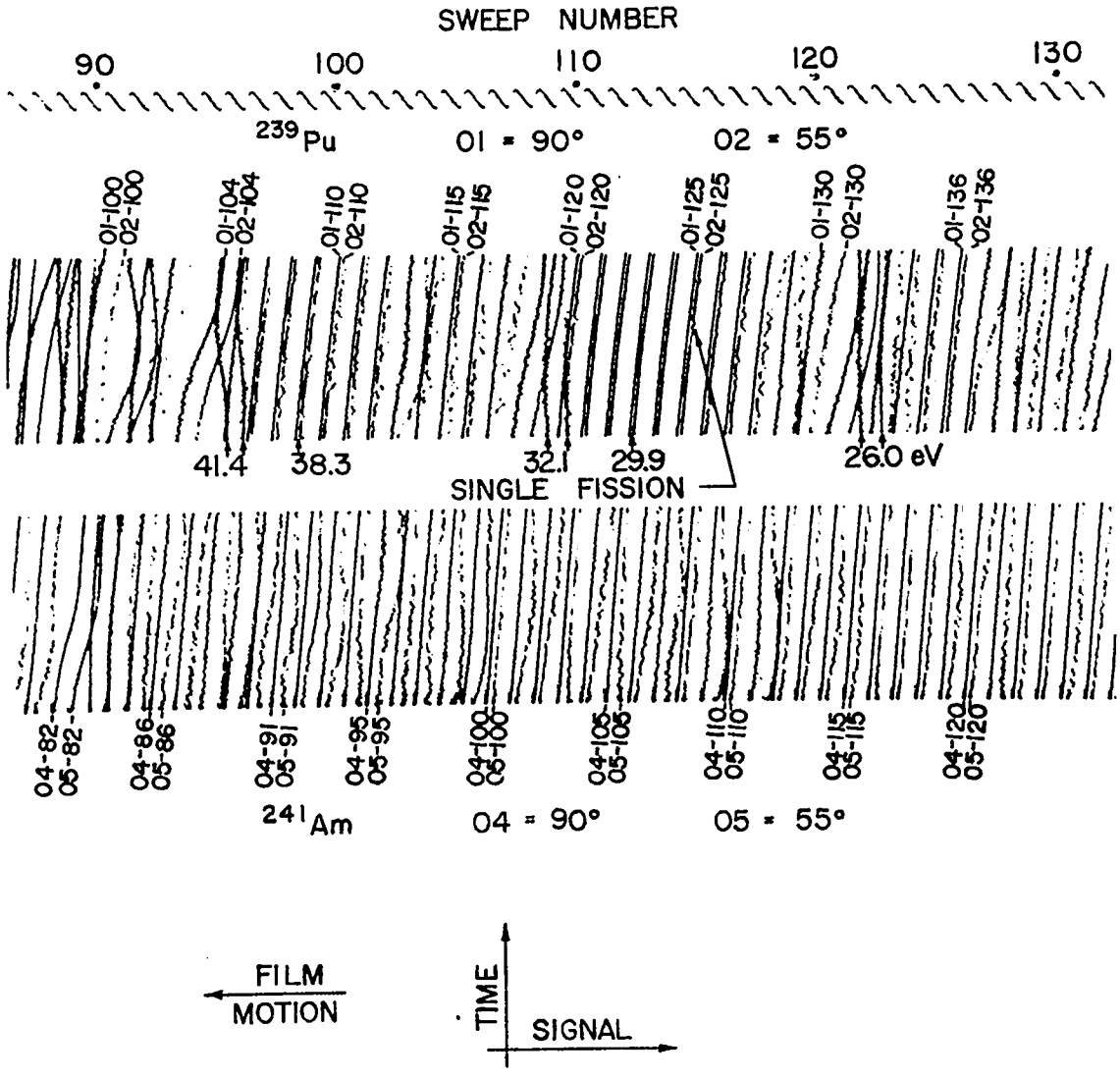

Fig. 3. Raster mode signals.

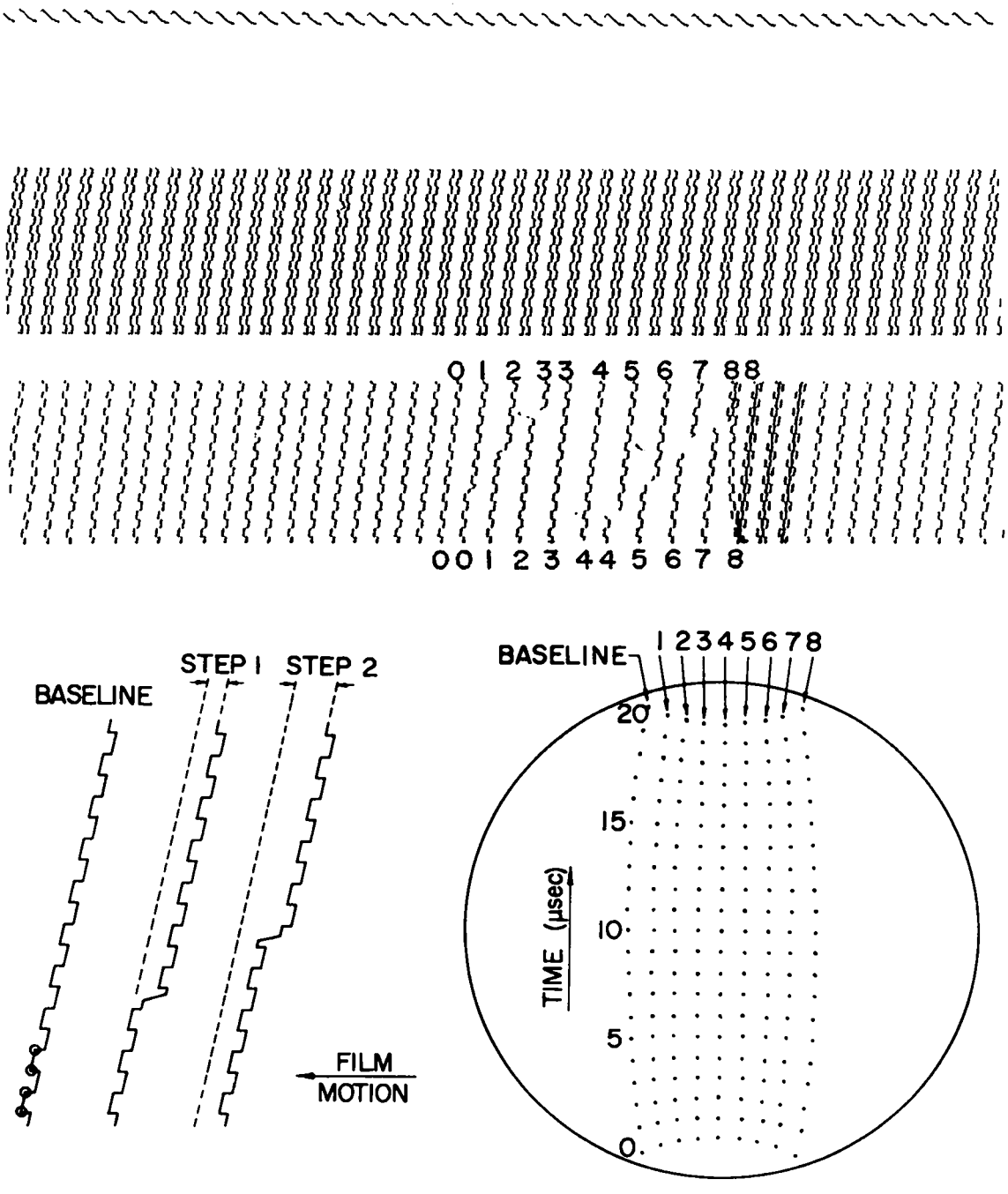

Fig. 4. Calibrations for raster mode signals.

record to be produced automatically by closing a switch. Manual operation involving the reading of a scale by an operator is prohibitive because of the large amount of data involved (~1.5×10^6 points, including multiple readings of all films). Travelling microscope systems, while minimizing optical distortion, are slower to operate and more tiring to the operator than projection microscope systems, and the latter have, therefore, been used almost exclusively as representing the best and most available compromise between speed and accuracy.

All films were read by LASL on a Richardson rear-projection machine with Datex digitizers and equipped to write magnetic tape. An independent set of readings onto punched cards was made at New Mexico State University on a Telereadex 29-E front projection system. Each digitizer had a unit size of approximately 1.5 μm. Since each data point is based on reading both the reference and the signal, the inherent reader error is on the order of 1% signal and far better than required in the time direction. The optimum rms reproducibility of the readings has proved to be about 4 μm at LASL and better than 3 μm at NMSU.

Some forms of distortion in the reader are compensated by reading the calibrations on the same machine. Other distortions are not removed and are a source of error in the final results; this source of error is included in the results as the rms deviations of the independent readings of the same signal. The NMSU machine has much less distortion than the LASL machine, as determined by comparing readings of the same portion of the signal trace made at opposite extremes of the viewing screen, such as the overlapping readings before and after advancing the film. (See the overlaps at 2200 μsec and 2500 μsec on Fig. 5 for bad and good examples of NMSU

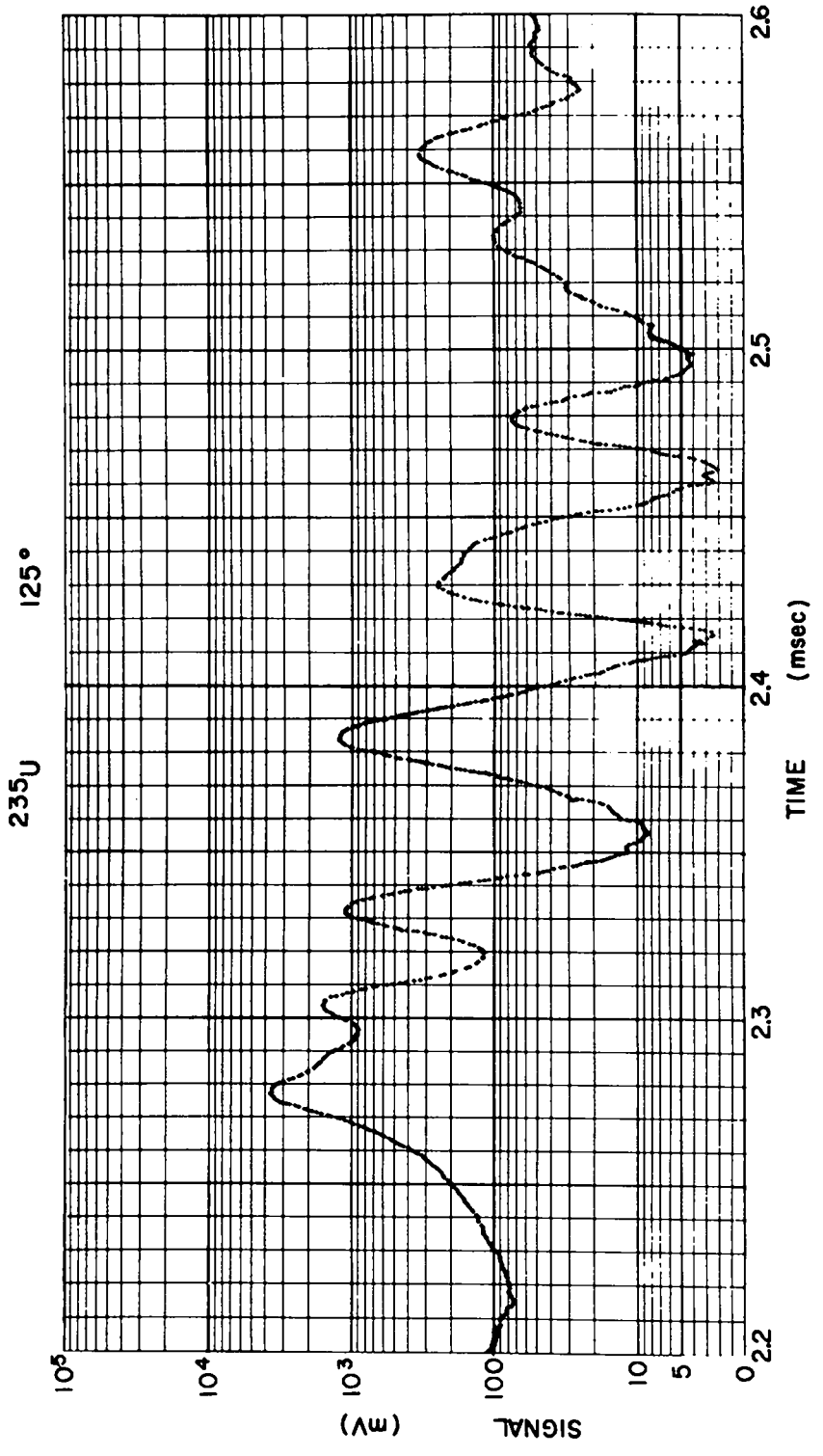

Fig. 5. A portion of the signal vs time output of program STRK, for ^{235}U.

readings.) Therefore, the NMSU readings have usually been given greater weight when several readings are averaged. In the worst cases, distortion leads to errors of the order of 5% (10-15 μm).

C. Automatic Film Reading

Programed-light-source film scanners are now available with a 5-μm diameter spot size addressable to about 1.5 μm. Such a machine will be able to read streak mode films very rapidly and with great uniformity and with a resolution of about 3 μm. Due to the complexity of the raster records, however, and the many crossings (see Fig. 4), it would be extremely difficult to program the reader to make the number of decisions necessary to follow the sweeps without operator assistance. Automatic reading is expected to be performed on streak records of future experiments. Additionally a high-speed drum camera which will be able to make streak mode recordings of the first 2 msec of the signals with time resolution equivalent to our current raster recordings, and which will be amenable to automatic reading, will be used on future experiments.

D. Editing and Preliminary Calculations

Since automatic readings have not been made on any films to date, only the procedures involved in analysis of semi-automatic readings are discussed.

Each point read from a film is converted to a 30 character card or tape record containing X-Y reader coordinates and book-keeping information (signal type, run, camera, signal, step number if calibration, and sweep number if raster). The

signal type was used to identify: 1) baseline, read before the onset of data and before the trigger for each calibration (see Fig. 2); 2) the signal; 3) baseline reference points (one such point was read at a similar position--the sharp corner before the rise--on each 20-μsec cycle of the baseline reference signal); and 4) the calibration. Four or five consecutive calibration staircases were read on most films.

As part of the editing procedure, the reference points are fit to equal time spacing by least-squares adjustment in the groups of 10 to 20 readings made without moving the film in the reader; it is not assumed that the X-reading is continuous when the film is advanced. Accurate X reference is particularly important for raster film, since the baseline is determined from it.

Calibrations and precalibration baselines are initially edited separately from the signals, and are processed by the appropriate programs (STRK or MVY2, see below) to determine the relationship of step 0 to the baseline. In the final edited tape, the records are in the order of calibrations (without their baselines), pre-signal baseline, and signal. The streak tapes are sorted in increasing order on X, so that the reference points are interspersed with the other readings. Raster tapes are sorted on sweep number and each sweep is sorted on the Y (time) readings; the first record for each sweep is the reference point reading.

III. Conversion to S(t)

The conversion of the digitized film information to S(t) is performed with Fortran codes (STRK for streak and MVY2 for raster films) on the LASL IBM 7094. These programs require, in addition to the digitized data, the mV levels of the calibration steps. These levels were determined under static conditions prior to the experiment; however, under the experimental conditions calibration difficulties were encountered: two such difficulties can be seen in the calibration examples of Fig. 2. First, during and following the closure of the commutator contacts for each amplifier, noise appeared on the line. This was due principally to improper grounding of the calibrator chassis, and for several amplifiers a dc level (determined by comparing the baseline to "step 0" just before step 1) appeared on the calibrator ground. Of the examples shown in Fig. 2, signals 20 and 17 had no such shift, but shifts of 1.3 mV and 1.1 mV occurred on signals 23 and 22, respectively, and these shifts had to be added to all steps, including "step 0." (This adjustment is referred to as "dc level.") The second difficulty is seen on signal 22: the commutator contact for signal 23 did not open until the second step of the signal 22 calibration. Because of the lower impedance then being driven by the calibrator output, the height of steps 1 and 2 above step 0 for signal 22 is just 2/3 of the measured value. Table I shows the values used in the programs as the step heights for these examples; for signals 20 and 17 they are just the measured values.

Table I

Calibration Step Heights

Step	Sig. 20,17 (mV)	Sig. 23 (mV)	Sig. 22 (mV)
0	0	1.3	1.1
1	2.5	3.8	2.8
2	7.2	8.5	5.9
3	20.5	21.8	21.6
4	57.7	59.0	58.8
5	163	164	164
6	458	459	459
7	1232	1233	1233
8	3625	3625	3625

A. Streak Film, Program STRK

The first readings placed on the input data tape are the calibrations. The program determines the average distance (Y-coordinate) of each step from the baseline reference trace, and the rms deviations of the readings for each step. The positions of the steps are then tabulated as the signal output levels in film-reader units corresponding to the mV levels read in on a card (e.g., from Table I), and the position of the 0 mV level is found by interpolation in the table. Next on the input tape are readings of the pre-signal baseline. These are averaged in the same manner; i.e., the separation in Y from the reference trace is found. To account for a possible difference in the position of the reference trace at calibration time due to hum, the positions of the calibration steps are then shifted so that the 0 mV level coincides with

the pre-signal baseline. (This adjustment is called "baseline shift.")

It is also proper to require the signal to return to 0 mV after the neutron flux has passed, about 3.5 msec after the onset of data. On some signals it was necessary to make a correction for 60 cycle noise ("hum") on the reference trace. Such correction was always taken to be linear with respect to time for the period over which data was accumulated; the largest hum correction made was 30 film reader units (45 μm) at 3.5 msec. Uncertainty in the hum can lead to uncertainties in the normalization of each signal of the order of ±10% below 50 eV.

The signal level of each point on the data tape can be found by comparing the distance of the signal point from the reference trace to the tabulated calibration-step positions. Linear interpolation is used for signals less than 5 mV, and logarithmic interpolation above 5 mV. Correction is then made for differentiation by the 0.75-sec time constant of the amplifier input; for strong signals the integrated charge on the input capacitor produced a maximum potential of 3 mV at late times. The amplifier contains a circuit which rapidly corrects for this input droop whenever the output level drops to zero; in the code this correction was accomplished by changing the time constant from 0.75 sec to 300 μsec. Because of the small size of the droop, uncertainties in this correction are negligible except in the lowest valleys between resonances.

The STRK program derives the time scale from the X-readings of the reference-trace points, which are interspersed on the input data tape with the signal readings. The zero of the time scale is arbitrarily set to the mark before the signal readings begin; as each reference reading is encountered, time is advanced by 20 μsec. The time corresponding to each signal reading is found by extrapolating from the last two

reference points read. The estimated rms error in time interval readings is ±0.3 μsec; this is negligible because it is less than the time resolution of streak mode recordings.

The output of STRK consists of listings of the calibration table, reference marks, and S(t); a magnetic tape containing S(t); and a set of graphs of S(t), such as shown in Fig. 5, which is a portion of the ^{235}U signal at detector angle 125^{o} as seen on the lowest trace in Fig. 1.

B. Raster Film, Program MVY2

Rather than separate signal and time calibrations to account for amplifier characteristics and non-linearities in the raster sweep generator, a two-dimensional calibration scheme was used which also corrected simultaneously for oscilloscope and camera distortions. Thus by identifying points of known times at several signal levels, or equivalently, by making signal level calibrations at several specific times across the sweep, a map of the distortions can be made. Figure 4 illustrates how this is done by superimposing a square wave on the amplifier output, and shows the possible appearance of the map in an extreme case.

The calibration readings are analyzed from the data tape as follows. The first reading for each sweep must be the reference-trace point for that sweep. This point is considered the origin of a complex number system in which the Y (time) reading is the real part and the X (signal) reading is the imaginary part. The time (μsec) corresponding to each point in a calibration sweep is just the index number of the point in the sweep, and the calibration step number was recorded when the original film was read. Thus the Y + i X reading for each point is averaged with previous readings of the same

point in the time and step array, and the rms deviations of the real and imaginary parts are also found and stored as another complex array.

Pre-signal baseline readings are next on the tape. (No examples are shown, but for practical purposes sweeps 121 through 124 of signals 01 and 02, Fig. 3, are baselines.) Again, the reference point for each sweep is first, and all readings are vectored from it. The baseline readings are used to determine the baseline position and also the trace slope, which will in general be different from the slope at calibration time because of a change of the film speed. (A negligible speed change occurs in the 4 msec of cross-section data.) As points on the baseline are encountered, they are compared to the location of zero signal level at the nearest time mark in the calibration array, and values for baseline shift are averaged together in the neighborhood of each time mark. The correction corresponding to the nearest time mark is applied to each signal reading.

Signal sweeps also must begin with reference trace readings. Time is arbitrarily set to zero at the beginning of the first sweep of signal readings, and advanced by 20 μsec for each sweep. For each point on a signal sweep, the closest point in the calibration array is found, along with the two appropriate "unit vectors" between neighboring points in the array such that the signal point is enclosed within the "unit square." Interpolation is performed by decomposing the vector from the closest array point to the signal point in terms of the unit vectors, since vectors between array points are in the direction of time and signal. Based on amplifier characteristics, interpolation in the signal direction is linear below and logarithmic above 5 mV.

Output for MVY2 is the same as for STRK.

IV. Determination of Cross Section

In the experiment under discussion, in which the detector-foil geometries are essentially identical for a number of foils and in which the neutron flux through all foils is the same, the relative cross section of one target to another is obtained quite trivially from a simple ratio. Thus if the cross section of the isotope contained on any one foil is known, all cross sections may be established relative to it. This procedure in a slightly more complicated form is used to determine the cross sections of foils in the nuclear device neutron time-of-flight experiments.

The usual reaction rate expression is used,

$$R = \sigma N f, \tag{1}$$

where R is the reaction rate, σ the cross section, N the areal density of target atoms, and f the incident flux. The observed signal is related to the reaction rate:

$$S(t) = R \cdot \frac{\Omega}{4\pi} \cdot e \cdot \bar{E} \cdot C + B(E) \tag{2}$$

where Ω is the solid angle subtended by, and e the efficiency of, the detector, $\bar{E}$ is the average energy of the detected particles, C is the conversion factor from the energy loss in the detector to mV signal level, and B(E) is the background signal level at the energy E corresponding to time t. It is important to note that since the final results involve ratios of two signals, the conversion factor C need not be known

precisely and only relative values of N, Ω, e, and $\bar{E}$ are required. The value used for C is 0.00242 mV-μsec-MeV^{-1}, based on 3.55 eV per ion pair in Si, electron charge = 1.6 x 10^{-13} μC, and a 53.6 Ω resistor at the amplifier input. The solid angle is always taken to be 0.12 sr, with any variations included in e.

The program SIGER, operating on the S(t) output as described in Sec. III, solves Eqs. (1) and (2) for either f or σ if the other is known, and also converts the time scale to energy. The time coordinates on the S(t) data tape are based on an arbitrary zero time. In transforming to an energy scale an accurate flight path and zero time are needed. The flight path is established prior to the experiment; on Petrel the flight path was set to the distance from the foil to the surface of a moderator located 40 cm above the nuclear device. This provided an accurate flight path for moderated neutrons but introduced a very small error for the direct neutrons of the fission peak. The zero time was adjusted to the arrival time of γ-rays (mid-point on the leading edge of the γ-flash peak) minus the flight time of 0.63 μsec. The relation used for energy conversion is

$$E = 5226.68\left(\frac{D}{t-t_o}\right)^2 \text{eV-}\mu\text{sec}^2\text{-m}^{-2}. \qquad (3)$$

where D is the flight path and $t-t_o$ the flight time. The SIGER program also averages the S(t) data in channels of fixed time width as this conversion is made. The time channel is usually 0.1 μsec for raster films and 1.0 μsec for streak films, but is lengthened by the program at low energies to approximately 1/8 the Doppler width (full width at 1/e). At temperature T for a target mass number A, this is

$$\Delta t = 2\sqrt{\frac{kT}{AE}}\, t \approx 1.6 \times 10^{-6}\ t^2.$$

The program SIGER subtracts a background and divides by a flux to obtain cross section. By varying the functions read into the computer for background and flux, the cross sections are derived following these procedures:

1) Establish background B(E). By setting "background" to 0 and "flux" to 1, the S(t) information from the desired signal (e.g., a blank target backing) is converted to signal (mV) vs energy (eV).
2) Establish flux. By setting background to B(E) and the "flux" to a known cross section (^{6}Li or ^{235}U), the S(t) from the detector viewing ^{6}Li or ^{235}U is converted to f(E).
3) Derive a partial cross section. Use B(E) for background and f(E) for flux. Appropriate values must be included for N, e, and $\bar{E}$.
4) Establish flux times cross section, g(E). By setting the background to B(E) from 1), "flux" to 1, and using appropriate values for N, e, and $\bar{E}$, the S(t) is converted to $g(E) = \sigma(E)f(E)$. This is used on flux monitors before transmission samples and before scattering foils.
5) Derive the total cross section from transmission. By setting the background to B(E) from 1), the "flux" to g(E) from 4), and inserting a value for sample thickness, with appropriate values for N, e, and $\bar{E}$ for the flux monitor following the transmission sample, the signal is converted to total cross section.

Figure 6 illustrates the results of using this program for converting S(t) for signal 20 (see "Background" trace in Fig. 1) to B(E). Figure 7 was obtained from the raster recording of signal 15 by using the known cross section of ^{235}U in the energy range 10^{4}-10^{6} eV to obtain flux and then using the flux to regain the cross section; the cross section used as the standard is shown as a line drawn through the statistically

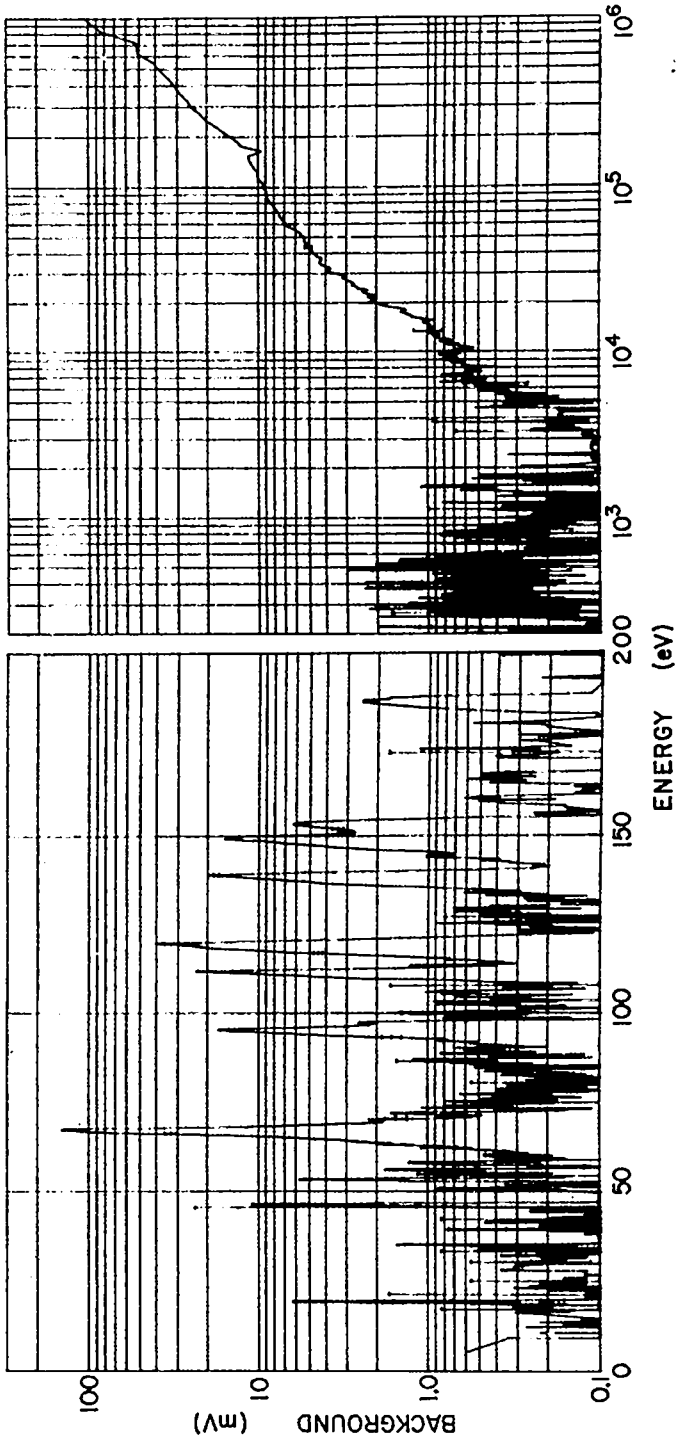

Fig. 6. Background signal for Petrel.

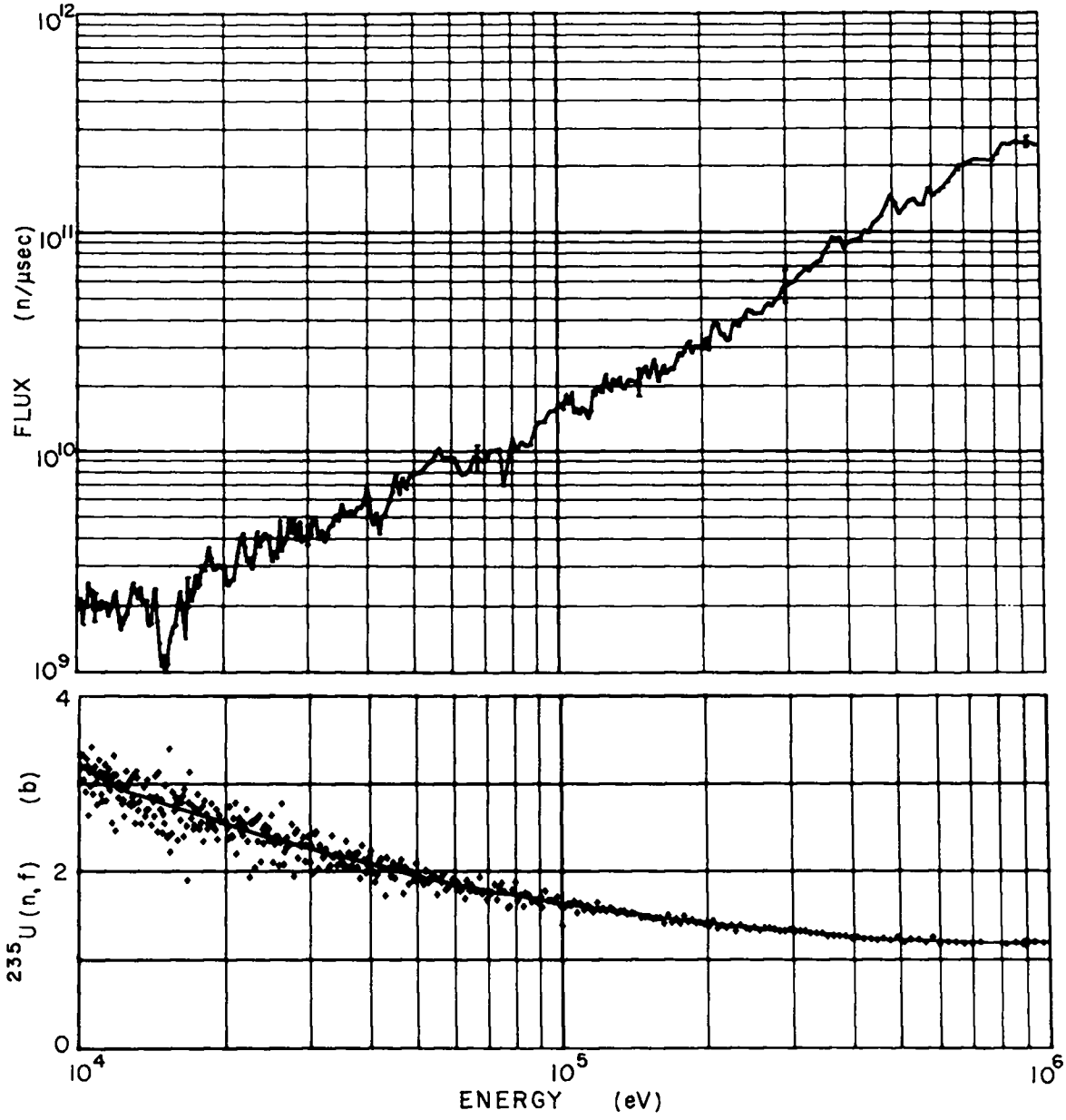

Fig. 7. High energy neutron flux and the ^{235}U data used in its derivation.

scattered points in the lower figure. Figure 8 shows the flux determined in the energy range 20 eV-10 keV obtained from raster and streak readings of signals 9 and 10, using the $^{6}Li(n,\alpha t)$ cross section as shown in the lower part of the figure.

A. Fission Cross Section

Target foil mass can be determined by chemical analysis combined with a determination of the foil isotopic composition by mass spectroscopy, by determining the alpha activity, or by comparing the thermal fission rate to a standard. Density N is then found by combining results of all measurements in the form of number of atoms and dividing by foil area; an additional factor of $\sqrt{2}$ enters because the foil is at 45^{o} to the beam. Table II includes the estimates of N for the targets used for fission measurements in Petrel, along with the estimated standard deviations, $\delta N/N$, of the determinations. The mass density of the deposit, an oxide in all cases except LiF, is also shown. The incident neutron beam fell completely within the target foil area except for the two Am targets;[2] for them the value of N has been multiplied by the fraction of the beam area utilized: the result is that for targets lying completely within the beam area, N is the total number of atoms divided by the beam area.

The size and efficiency differences between charged particle detectors was determined by measuring the counting rate for each detector when exposed to a radioactive source under identical geometry conditions. Such differences are treated as detector efficiency e; all signals are normalized to the flux detector. In addition to the actual counter efficiency, the factor e includes the effect of the beam being

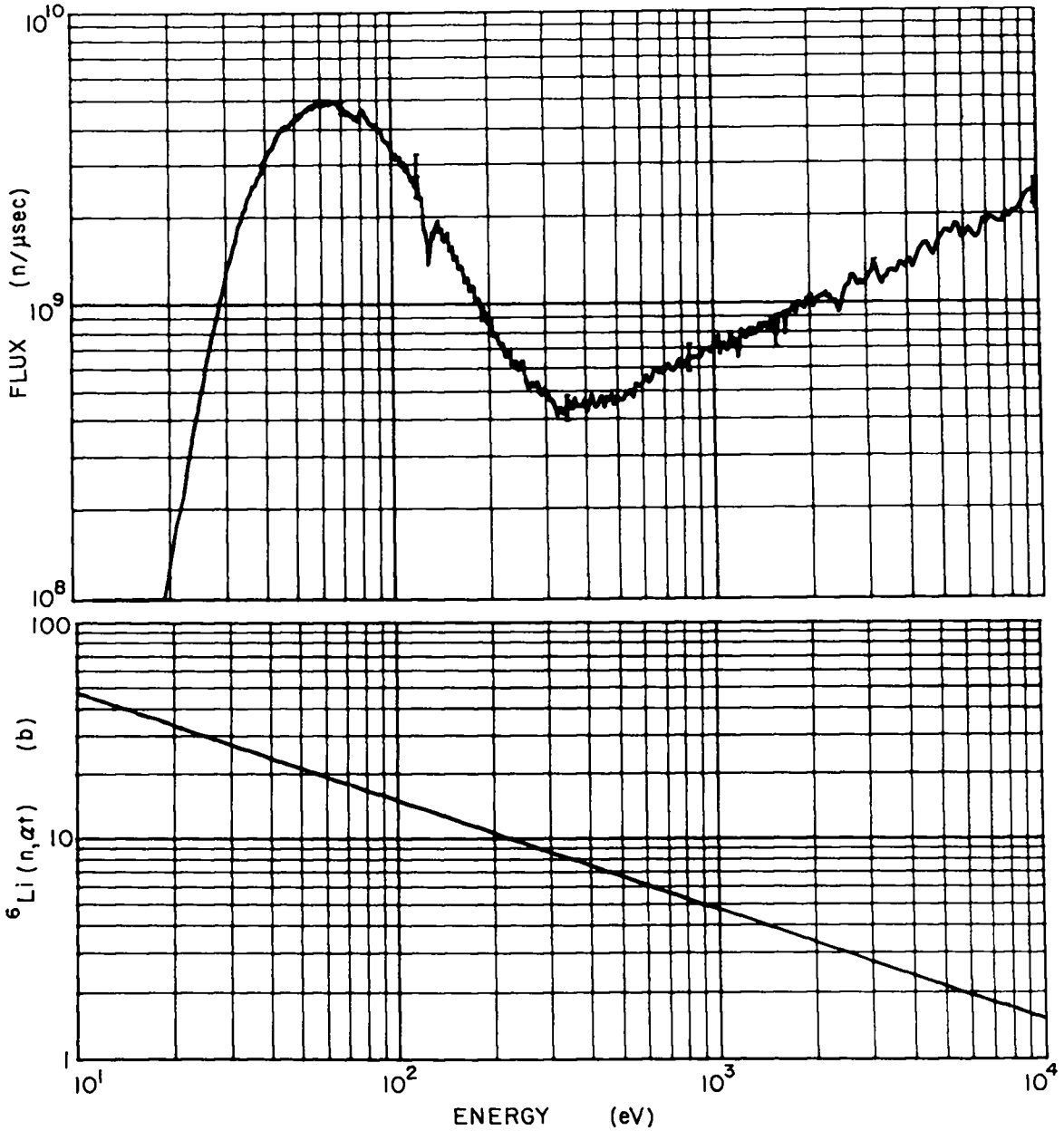

Fig. 8. Low energy neutron flux as derived from ^{6}Li.

Table II

Factors Involved in Normalization and Determination of Errors

Target	Foil Density Normal to Surface (mg/cm^2)	N (atoms/barn)	$\delta N/N$	e	$\delta e/e$ Referred to ^{6}Li	$\delta e/e$ Referred to ^{235}U	Q (MeV)	δQ (MeV)	$\bar{E}$ (MeV)	$\delta\bar{E}/\bar{E}$	$\delta\bar{E}/\bar{E}$ Referred to ^{235}U	Correlated Error Referred to ^{6}Li	Correlated Error Referred to ^{235}U
Fission													
^{6}Li	0.511	1.670×10^{-5}	0.05	1	0	0.028	4.787		--		0.035	0	0.064
^{233}U	0.519	1.632×10^{-6}	0.03	1.022	0.022	0.028	173.1	0.1	42.4	0.045	0.038	0.079	0.060
^{235}U	0.586	1.864×10^{-6}	0.02	1.030	0.028	0	171.5	0	48.2	0.035	0	0.072	0
^{239}Pu	0.492	1.545×10^{-6}	0.03	1.007	0.028	0.045	181.5	1.2	54.0	0.033	0.030	0.073	0.065
^{240}Pu	0.587	1.833×10^{-6}	0.05	1.007	0.036	0.028	180.7	1.1	52.0	0.035	0.031	0.087	0.068
^{241}Pu	0.526	1.563×10^{-6}	0.05	0.994	0.022	0.022	179.9	1.1	51.6	0.035	0.031	0.078	0.065
^{241}Am	0.425	5.73×10^{-7}	0.02	0.974	0.022	0.036	186.6	1.8	55.8	0.037	0.031	0.071	0.057
^{242}Am	0.253	7.72×10^{-8}	0.03	0.950	0.036	0.022	185.8	1.8	54.5	0.037	0.032	0.079	0.054
Capture													
^{233}U	441.	1.63×10^{-3}	0.05	0.038	0.16	0.16	6.77	0.11	0.150	--	--	0.175	0.169
^{240}Pu	318.	1.14×10^{-3}	0.02	0.031	0.06	0.06	5.52	0.10	0.150	--	--	0.081	0.066

off the center line of the target array, due either to a shift or tilt of the vacuum box. The beam was determined to have been 0.1 in. off center at the top of the box, and tilt has been assumed. The maximum solid angle change is then 4%; an estimated error of 1% per target position away from the standard has been assumed. Another factor entering into e is that of time dilation resulting from using flux per unit time which for a given energy varies with source distance. The efficiency factor e has been multiplied by the ratio of the distances to the target in question and to the ^{6}Li target. The resulting values for e and $\delta e/e$ as referred both to ^{6}Li and to ^{235}U are shown in Table II.

The average fragment energy, $\bar{E}$, deposited in the detector depends on the Q-value and the foil and dead layer thickness. $\bar{E}$ was determined experimentally for detector thicknesses between 0.9 and 3.1 μm by bombarding the ^{235}U foil used on the Petrel experiment with thermal neutrons, recording the fragment energy spectra and deriving the average energy. The Q-values for the fissile targets, also important to the center-of-mass correction, were calculated according to the mass law[3] equation,

$$Q = 0.22\ Z^2/A^{1/3} - 3.4\ A^{2/3}\ , \qquad (4)$$

and are shown in Table II. The errors $\delta Q/Q$ shown there are relative to ^{235}U as a standard, and were calculated on the basis of 10% errors in each of the two coefficients in the expression for Q. Using this Q for ^{235}U, the empirically derived expression for $\bar{E}$ in MeV is

$$\bar{E} = Q/2 - 17.3 - 8.8\ d \qquad (5)$$

where d is the detector window thickness in μm. The error in the calculated $\bar{E}$ is due to the error in Q/2, an error of ±0.1 μm in window thickness d, and the error (with correlation) in the two derived coefficients:

$$(\delta\bar{E})^2 = (\delta Q/2)^2 + (0.88)^2 + (0.38d^2 + 0.81d + 1.92)\cdot(0.6)^2. \quad (6)$$

In the last term of this expression, 0.6 MeV is taken as the standard deviation of a single determination of $\bar{E}$ in the thermal neutron experiment. Values of $\bar{E}$ and $\delta\bar{E}/\bar{E}$ are given in Table II. When the error is referred to ^{235}U, another term of 0.88 MeV enters in Eq. (6) for the uncertainty in the ^{235}U detector window, but the d used is the absolute difference between the d of the detector and that of the ^{235}U detector.

For ^{6}Li, Q = 4.787 MeV and $\bar{E}$ is calculated from energy loss measurements[4] of α and t in LiF. Measurements of α stopping in Si indicate that a Si atom has essentially the same stopping power as LiF; therefore, the number of Si atoms/cm^2 in the detector window has been added to half the number of LiF molecules/cm^2 in the foil for the energy loss calculations. The calculations were tested with a thermal neutron beam, the LiF foil used in the Petrel experiment, and five different detector window thicknesses, and found to agree within experimental errors. An error was assigned of 10% of the calculated energy loss. As this error varies with incident neutron energy, it has not been included with constant sources of correlated error, but rather has been incorporated into the statistical error of the flux determination.

B. Capture Cross Section

Target foil masses were determined using the appropriate techniques listed in Paragraph A.

The efficiency for γ-ray (Moxon-Rae type) detectors was determined in two ways: (1) normalizing to $(1 + \alpha)\cdot\sigma_f$ at the peak of a wide resonance (i.e., small $\alpha = \sigma_c/\sigma_f$) in ^{233}U; and (2) computing $e\cdot\bar{E}$ at a black resonance in ^{240}Pu. In the first case the value of $e\cdot\bar{E}$ is obtained directly from Eq. (2) by setting $\sigma = (1 + \alpha)\cdot\sigma_f$ and considering $e\cdot\bar{E}$ as a free variable. In the second case R is set to $a\cdot F$ where a is the relative blackness of the resonance and $e\cdot\bar{E}$ is derived from Eq. (2). The two results agree well when expressed as efficiency/MeV of γ. For computation purposes a value of 150 keV was assumed for $\bar{E}$ for the conversion electrons, based on a few electron spectra measurements made on the Moxon-Rae type converters. The value is required for the average electron energy deposited in the detector for determining the statistical error. The value of e used in the computations is listed in Table II. Note that for isotopes which both fission and capture, the relative efficiency of the γ-ray detectors to fission and capture γ-rays has been assumed to be one; the results of this computation are thus $\sigma_f(E) + \sigma_\gamma(E)$.

C. Scattering Cross Section

If a neutron detector with uniform efficiency is used, the analysis would be the same as for fission cross sections, with $\bar{E}$ determined appropriately. A different situation arises if the same reaction is used to detect scattered neutrons as is used to measure the flux in the beam, e.g., $^{6}Li(n,\alpha)t$.

In that case the cross section of the reaction does not enter the calculation. Instead of being divided by flux, the signal is divided by the product of cross section times flux, determined by procedure 4) above. The factor $\bar{E}$ is that appropriate to the detecting reaction, and the factor N is the areal density of the scatterer. The detection efficiency e, in addition to the usual factors, must also be multiplied by the solid angle ratio for detecting the charged particles (unity for reactions in which two particles are emitted and the foil is deposited on the detector surface), and also by the number of atoms per unit area in the detector foil deposit. Thus e has units of inverse cross section, so that $eg = e\sigma f$ has units of flux.

D. Total Cross Section

The experiment consists of a flux-measuring foil (e.g., ^{6}Li), followed in the beam by an absorber, followed in turn by a second flux measuring foil of the same material as the first. By procedure 4), the product $g_1 = \sigma f_1$ can be found for the first foil; the ratio $f_2/f_1 = g_2/g_1$ could also be found. As indicated in procedure 5), however, the program SIGER will convert this transmission ratio into cross section if a value is given for the reciprocal thickness 1/N (barns per atom) for the sample:

$$\sigma_T(E) = \frac{1}{N} \ell n\left(\frac{g_1}{g_2}\right) \quad . \qquad (7)$$

The statistical errors in g_1 and g_2 are found from the respective counting rates, background subtractions, and errors

in $\bar{E}$, and the statistical error in σ_T by

$$\delta\sigma_T = \frac{1}{N}\left[(\delta g_1/g_1)^2 + (\delta g_2/g_2)^2\right]^{\frac{1}{2}} .$$

V. Treatment of Errors

The sources of systematic error were discussed in the preceding section and listed in Table II, where they are also combined into the total correlated error, referred both to ^{6}Li (for use below 10^4 eV) and to ^{235}U (for use above 10^4 eV). Note that in the tabulation of the fission data in LA-3586[5] and also on the SCISRS data tape, the error referred to ^{6}Li was used throughout. Also note that the correlated errors now calculated for the U isotopes are reduced, because of better estimation of the uncertainties in $\bar{E}$. This is particularly true for ^{233}U, for which the detector had the greatest window thickness.

Sources of error which vary with energy or signal level are included with the statistical error. These include the rms deviations of the calibration steps due to both reading error and calibrator jitter, $\delta\bar{E}/\bar{E}$ for ^{6}Li, statistical errors of the points, and errors in background subtraction and flux determination. The statistical error of a point is determined by converting the sum of all input signals in a time channel to counts and comparing the statistical error of this number to the rms deviation of the signal for all points in the time channel; the larger of the two is taken as the statistical error.

Independent readings of the same signal are averaged and graphed by the GRAV program. In this process the corre-

lated error is removed and points are weighted inversely as the square of the statistical error; arbitrary weighting factors may also be applied. An internal error is calculated as the square root of the weighted sum of the squares of the statistical errors of the individual readings, and an external error as the square root of the weighted mean of the squares of the deviations from the average. The statistical error of the result is set to the larger of the calculated internal and external errors and recombined with the correlated error. Figure 9 displays the GRAV output for the average of three readings of streak signal 15 (bottom trace in Fig. 1) over the energy interval 28-38 eV, which is essentially the same interval shown as S(t) in Fig. 5.

VI. Conclusion

The final result of the data analysis procedures described in this report is an experimental cross section as a function of energy. Up to this point, no corrections have been made for neutron-source and electronic-resolution functions, for target thickness (insignificant for fission measurements), or for target impurities. The fission data for Petrel are presented in LA-3586[5] and in a series of papers.[2,6-10] Note that for ^{240}Pu, ^{241}Am, and $^{242}Am^{m}$ the impurity corrections have been made. Capture cross section measurements on ^{233}U and ^{240}Pu will be reported further.[11,12] The scattering and transmission experiments on Petrel were of an exploratory nature only; no results will be reported.

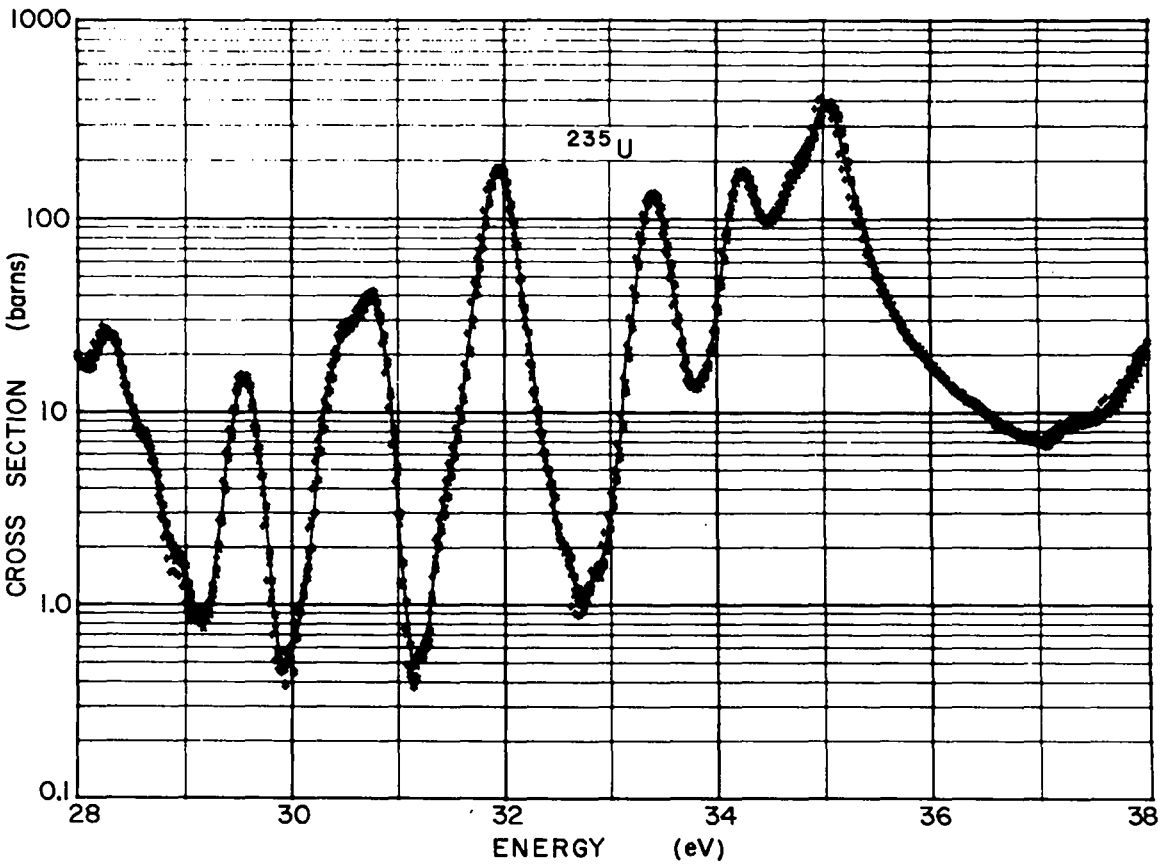

Fig. 9. Cross section (output of program GRAV) for the portion of ^{235}U data shown in Fig. 5.

References

1. A. Hemmendinger, B. C. Diven, W. K. Brown, A. Ellis, A. Furnish, and E. R. Shunk, Los Alamos Scientific Laboratory report LA-3478, Part I, to be issued.
2. P. A. Seeger, A. Hemmendinger, and B. C. Diven, Nucl. Phys., to be published.
3. P. A. Seeger, W. A. Fowler, and D. D. Clayton, Astrophys. J. Suppl. XI, 121 (1965).
4. W. Whaling, Encyclopedia of Physics, Springer-Verlag, Berlin, 1958, p. 193.
5. Los Alamos Scientific Laboratory report LA-3586, 1966.
6. D. W. Bergen, M. G. Silbert, and R. C. Perisho, Conference on Neutron Cross Section Technology, Washington, D.C., 1966, report CONF-660303, p. 895.
7. W. K. Brown, D. W. Bergen, and J. D. Cramer, op. cit., p. 971.
8. E. R. Shunk, W. K. Brown, and R. LaBauve, op. cit., p. 979.
9. D. H. Byers, B. C. Diven, and M. G. Silbert, op. cit., p. 903.
10. O. D. Simpson, R. G. Fluharty, M. S. Moore, N. H. Marshall, B. C. Diven, and A. Hemmendinger, op. cit., p. 910.
11. D. W. Bergen, to be published.
12. D. H. Byers, to be published.